Loading rate dependence of the fracture toughness of polycrystalline tungsten: Experiments and Modeling

Daniel. Rupp[1,a], Xiaohui Zeng[2,b], Sabine M. Weygand[1], Alexander Hartmaier[2]

[1] Institute for Material Research II (IMF II), Forschungszentrum Karlsruhe in der Helmholtz-Gemeinschaft, Herrmann-von-Helmholtz-Platz 1, D-76344 Eggenstein-Leopoldshafen, Germany

[2] Center for Advanced Materials Simulation (ICAMS), Ruhr-University Bochum, Stiepeler Str. 129 (UHW), 44780 Bochum, Germany

[a]daniel.rupp@imf.fzk.de, [b]xiaohui.zeng@ww.uni-erlangen.de

Keywords: Fracture toughness, brittle-to-ductile transition, polycrystalline tungsten, transition temperature

Abstract. In the experimental part we have investigated the fracture toughness and the brittle-to-ductile transition of polycrystalline tungsten. Like most technological materials, our starting material possesses an anisotropic microstructure caused by the production process. Thus, special attention has been drawn to the dependence of fracture toughness and fracture behavior on the crack orientation. Our work aims at generating a comprehensive data set of the fracture toughness of polycrystalline tungsten as a function of temperature, loading rate and crack orientation over the entire range from brittle to ductile response.

In a numerical approach, we employ a combined two-dimensional dislocation dynamics / cohesive zone model to describe crack-tip plasticity and to predict the fracture toughness. The results show that it is essential to take the effect of the confinement of the plastic zone introduced by grain boundaries into account to capture the rate dependence of the fracture toughness correctly.

Introduction

Body centered cubic metals like tungsten fail generally by brittle fracture at low temperatures. With increasing temperature, a pronounced transition from brittle to ductile fracture behavior can be observed. The fracture toughness and its dependency on temperature, crack orientation and loading rate has been studied extensively for single crystalline tungsten [1,2], while data of polycrystalline tungsten are still rare. Particularly for brittle metals, the microstructure plays a decisive role for the fracture behavior and the resulting fracture toughness. Thus, a detailed understanding of the micro-mechanisms controlling the fracture process and their interaction with the microstructure is crucial to identify ways of improvement for technological applications.

Polycrystalline tungsten is usually produced by a powder metallurgy route and is commercially available in many forms. The variation in the experimental data of recently published works [3,4] concerning the brittle-to-ductile transition temperature (BDTT) of polycrystalline tungsten and tungsten alloys exhibits again the strong influence of the production process. With our experimental programme we aim at generating a comprehensive data set of the fracture toughness of polycrystalline tungsten as a function of temperature, loading rate and crack orientation over the entire range from brittle to ductile response similar to the already available one for tungsten single crystals [1,2]. In this work, we focus on a very common variety, namely sintered and rolled tungsten rods, which exhibit a pronounced texture. Specimens were extracted in three different directions and have been tested under three point bending, which shows the influence of texture and crack orientation. Furthermore, we have started to vary the applied loading rate. In the future we will continue with the investigation of the loading rate dependency of fracture toughness and the brittle-to-ductile transition (BDT).

Fig. 1 illustrates the crack problem studied in the present work. A long sharp crack subjected to mode I loading is represented by virtual dislocation dipoles. A single crack-tip source is positioned near the crack tip. The slip plane, corresponding to the maximum resolved shear stress, is inclined by 70.5° with respect to the crack line. Grain boundaries are introduced as impenetrable obstacles for dislocations so that the shielding dislocations may pile up against the boundary. Consequently, the plastic zone is confined by the grain boundary and the fracture toughness becomes a function of the grain size. Crack propagation is described by a cohesive zone (CZ) model. For more detailed information of the methodology, the readers are referred to [5,6].

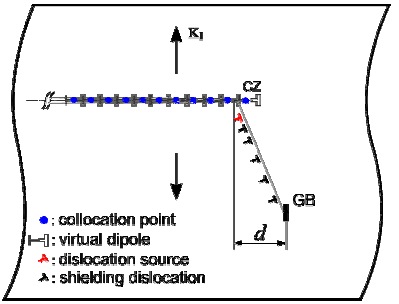

Fig. 1. A long crack situated in an infinite isotropic elastic solid loaded with stress intensity factor K_I. Dislocations are emitted from the single dislocation source (marked in red color) and glide on a single slip plane, which corresponds to the maximum resolved shear stress. r_{tip}: crack-tip blunting radius; d: grain size defined by the distance between the crack tip and the grain boundary (GB).

Experimental procedure

Material and microstructure. The starting material, which has been chosen for our studies on polycrystalline tungsten, are rolled unalloyed 99.98% pure tungsten rods with a diameter of roughly 14 mm. This commercial material was produced by Plansee Metall GmbH, Reutte/Austria, in a powder metallurgical route. After sintering the rods experienced a break down rolling with a degree of deformation of 65%. The resulting microstructure exhibits elongated grains with an aspect ratio of roughly 1:3 in the rolling direction (see Fig. 2(a)). Additionally, the elongated grains possess a preferred orientation regarding the rolling direction, namely a <110>-fiber texture (see Fig. 2(b)).

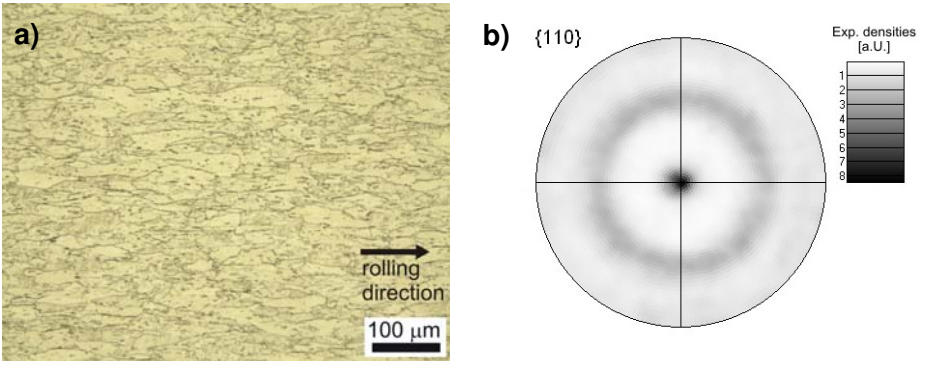

Fig. 2. a) Optical micrograph of a longitudinal section. The micrograph shows elongated grains along the rolling direction with an aspect ratio of roughly 1:3. b) {110}-pole figure showing the <110>-fiber texture. The pole figure was measured by means of EBSD on a cross section perpendicular to the rolling direction.

Close investigations by means of Electron Back Scatter Diffraction (EBSD) showed that the fiber texture is especially pronounced in the center of the rods. Thus, the bending specimens (3x6x27mm) were only extracted from the center of the rolled rods using Electrical Discharge Machining (EDM). Furthermore, the orientation images at higher magnification exhibit that a low angle cell structure inside the grains has formed due to the high degree of deformation.

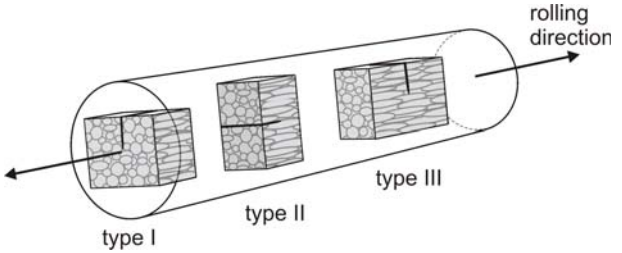

Fig. 3. Indication of crack orientation and texture of the investigated specimens: in the first case is the crack front parallel (type I), in the second one radial (type II) and in the third case tangential (type III) to the rolling direction.

To account for the anisotropic microstructure the specimens are extracted in three different kinds of crack orientations (see Fig. 3). : in the first case is the crack front parallel (type I), in the second one radial (type II) and in the third case tangential (type III) to the rolling direction.

As the transverse specimens (type I, II) are limited in their size, they needed to be brazed to two extension arms to obtain the desired geometry. The brazing process was carried out in high vacuum of $5x10^{-5}$mbar at a temperature of 1050°C for half an hour using a Nickel based brazing alloy (STEMET 1311) [7]. The comparison of the optical micrographs of a sample in the initial and the annealed condition revealed no influence of the brazing process. Furthermore, no change in Vickers hardness (429 HV30) and in fracture toughness could be observed.

Fracture mechanical testing. To obtain the fracture toughness notched specimens were tested in 3-point-bending. The notches were produced in the following way: first 3mm deep notches were cut into the specimens by EDM. Afterwards, the notches were extended with a common method for fracture toughness tests of ceramics where a razor blade is used [8]. The resulting notches possess a well-defined tip radius of roughly 20µm and an overall notch depth of about 3.2mm (see Fig. 4).

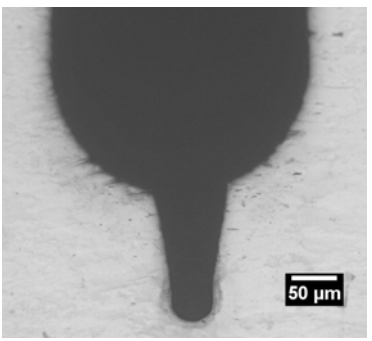

Fig. 4. Optical image of the tip of a notch used for the fracture mechanical tests. The notches were introduced by the method described in the text.

Two different universal testing machines were used depending on the test temperature while the geometry of the bending setups was identical in both machines. For the tests at lower temperatures, a servohydraulic testing machine with a climate chamber was used. The specimen temperature within the chamber could be adjusted in a range from -150°C up to 350°C by cooling with gaseous nitrogen and by a resistance heating respectively. Above 350°C, an electromechanical testing machine equipped with a vacuum chamber and a resistance heating was used. All tests were conducted in displacement control at fixed traverse speeds; the displacement of the loading point was directly measured by an additional extensometer. The fracture toughness K_{IC} has been calculated following the ASTM E399 standard using the notch depth as crack length. The comparison of notched specimens to specimens with a sharp precrack and the effect on the BDT will be addressed in future studies.

Results and Discussion

Fracture toughness and BDT. Fig. 5(a) shows the fracture toughness as a function of temperature for all 3 crack orientations. The tests were made at a fixed loading rate of 1µm/s which corresponds to a stress intensity rate of about $\dot{K} = 0.5$ MPa $m^{1/2}s^{-1}$. With increasing temperature fracture toughness raises for all three types and a transition from brittle to ductile fracture behavior can be observed. A distinct anisotropy of fracture toughness and its dependency on temperature can be observed. The longitudinal specimens (type III) extracted in the rolling direction exhibit much higher fracture toughness than the type I and II specimens over the investigated temperature range. Whereas both transverse specimen types show almost the same fracture toughness at room temperature, the type I specimens are more brittle than the type II specimens at elevated temperature.

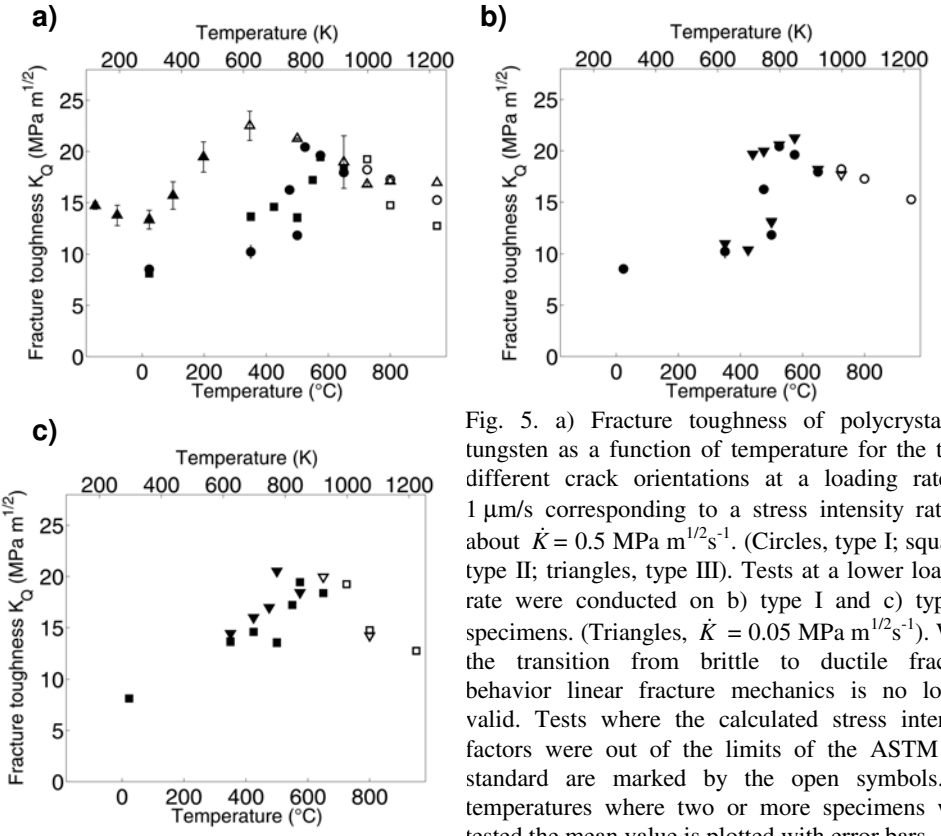

Fig. 5. a) Fracture toughness of polycrystalline tungsten as a function of temperature for the three different crack orientations at a loading rate of 1 µm/s corresponding to a stress intensity rate of about $\dot{K} = 0.5$ MPa $m^{1/2}s^{-1}$. (Circles, type I; squares, type II; triangles, type III). Tests at a lower loading rate were conducted on b) type I and c) type II specimens. (Triangles, $\dot{K} = 0.05$ MPa $m^{1/2}s^{-1}$). With the transition from brittle to ductile fracture behavior linear fracture mechanics is no longer valid. Tests where the calculated stress intensity factors were out of the limits of the ASTM test standard are marked by the open symbols. At temperatures where two or more specimens were tested the mean value is plotted with error bars.

As can be seen in Fig. 5(a) the transition from semi-brittle to ductile fracture behavior of type I and II specimens occurs in the region between 475 and 575°C. Compared to the two transverse specimens, the type III specimens show a significantly lower transition temperature at roughly 250°C. Furthermore, the type I specimens where the crack front is parallel to rolling direction exhibit a more pronounced transition in a smaller temperature range than the other two types, As a consequence of the scatter in the experimental data, particularly in the range of the transition, more tests will be conducted to quantify the results.

To study the loading rate dependence, first experiments were made at a lower loading rate of 0.1 µm/s corresponding to a stress intensity rate of about $\dot{K} = 0.05$ MPa $m^{1/2}s^{-1}$. The results for the type I and II specimens are shown in Fig. 5(b) and c) respectively. As can be seen, the transition of both types is shifted to lower temperatures with decreasing loading rate.

Compared to the single crystal data of Gumbsch et al. [1,2] where the loading rate was also varied over one decade, the polycrystalline material responds much less sensitive to the variation of the loading rate. This finding is consistent to the results obtained from numerical simulations as will be shown later.

Fractography. To gain insight into the responsible fracture mechanisms the fracture surfaces of tested specimens have been extensively examined by scanning electron microscopy (SEM). Fig. 6 shows selected fractographs to give a brief overview of typical fracture morphologies that could be observed. Fig. 6(a) and (c) show the fracture surfaces of type I and II specimens tested at room temperature. The fracture morphology of both types is dominated by intercrystalline fracture; however, some grains failed by transcrystalline cleavage. No significant change of the fracture morphology could be observed for temperatures below room temperature and up to 800°C. At 950°C, the fractographs of both transverse types showed locally some micro-ductility (Fig. 6(b) and (d)).

The longitudinal specimens (type III) exhibited a completely different fracture behavior below 350°C. As shown in Fig. 6(e), the specimens failed by almost pure cleavage at room temperature. Transcrystalline fracture could scarcely be observed. With increasing temperature, a significant change of the fracture behavior occurred; the specimens did not fail anymore along their symmetry plane, but a crack emerged about 200 µm below the notch and parallel to the rolling direction (Fig 6(f)). The examination of the fracture surfaces revealed that whereas this crack grew by intercrystalline fracture along the grain boundaries in the rolling direction, the region between the notch and the crack failed by ductile fracture. Our first experiments conducted on specimens with a sharp precrack exhibit the same fracture behavior at these temperatures. At 950°C finally, only blunting of the notch tip could be observed.

Modeling. All numerical experiments are performed at room temperature and at constant loading rate $\dot{K}$ for single- and poly-crystals of tungsten. The monotonic crack growth simulations are terminated when a complete decohesion between the cohesive surfaces of the first element in the cohesive zone occurs. For the single source model, this decohesion leads to a continuous crack propagation without further loading because there are no surrounding dislocations in the vicinity of the advancing crack tip to relax the enhanced stress concentration. The remote loading stresses at the termination points are collected as the critical stress σ_{crit} at fracture. For a sharp or slightly blunted crack such a stress translates into a critical stress intensity factor (or fracture toughness) through $K_{crit} = \sigma_{crit} (\pi a)^{0.5}$, where a is the crack length. The values for material and model parameters for room temperature were chosen from [6] and [9].

Fig. 7 shows the fracture toughness as a function of loading rate and grain size for both a sharp crack and a slightly blunted crack. The model correctly predicts the fact that fracture toughness increases with decreasing loading rate. It is also found that the fracture toughness decreases with grain size. As mentioned above the grain size limits the length of the dislocation pile-up. For fine-grained materials one may expect improved elastic shielding because the dislocations stay closer to the crack-tip. However, these dislocations also cause a back stress on the dislocation source. When the back stress becomes sufficiently high, the dislocation source will be blocked. The locking of the dislocation source limits the number of dislocations and also the plastic strain rate and thus causes an embrittlement of the material. It is also seen that the grain size effect depends on the loading rate. For the lowest loading rate investigated here, the fracture toughness significantly decreases from the largest grain size to the smallest one.

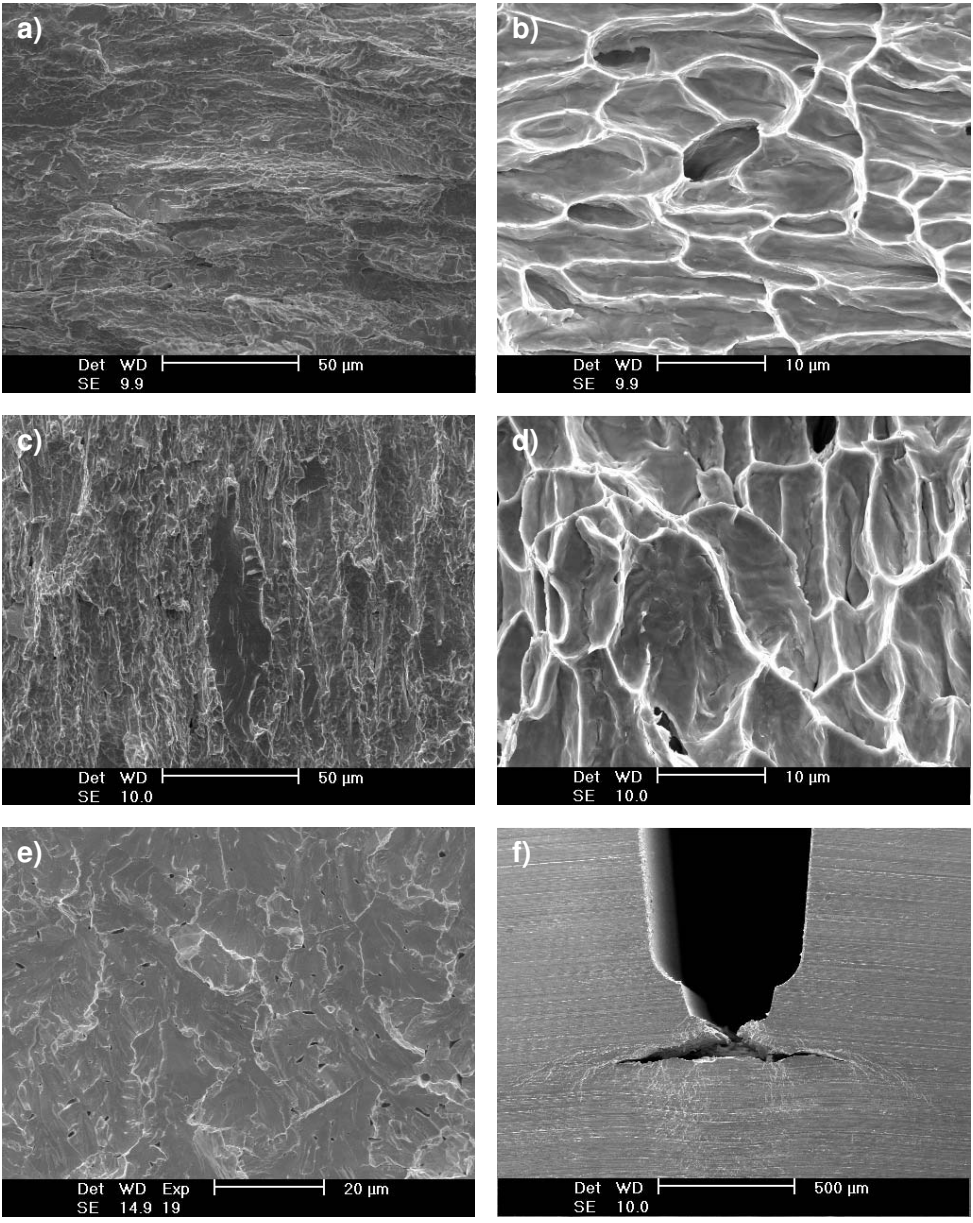

Fig. 6: Fractographs of tested specimens. SEM images of type I specimens fractured at a) room temperature and b) 950°C. Type II specimens at c) room temperature and d) 950°C. Type III specimens at e) room temperature and f) 650°C.

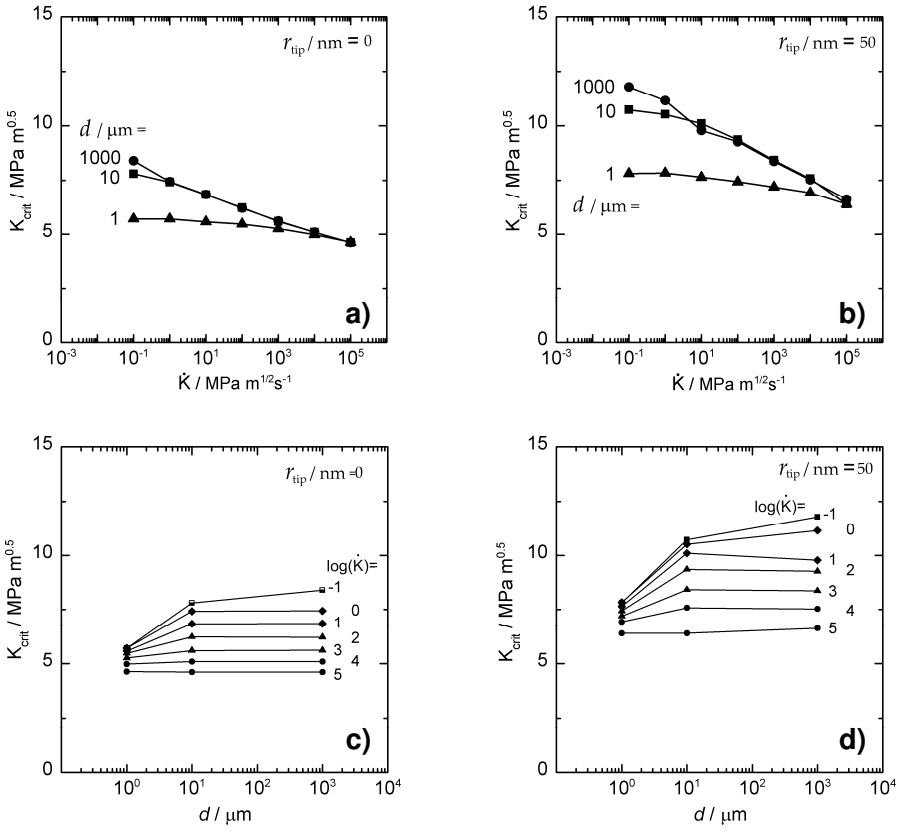

Fig. 7: Fracture toughness as a function of loading rate and grain size d for sharp cracks (r_{tip} = 0 nm) (a) and (c) and slightly blunted cracks (r_{tip} = 50 nm) (b) and (d). Simulations are done for three different grain sizes of 1, 10 and 1000 µm at room temperature. Loading rate $\dot{K}$ is given in MPa m$^{1/2}$s^{-1}.

With decreasing grain size (or increasing loading rate) the lengths of pile-ups and hence the number of dislocations becomes smaller, which leads to reduced fracture toughness. For large grain sizes (or high loading rates) the dislocations are not able to reach the grain boundary before fracture occurs, and thus no confinement of the plastic zone occurs and fracture toughness is independent of grain size in that case. The confinement of the plastic zone by the grain boundaries also explains the observation (see Fig. 7(a) and (c)) that the large-grained materials have higher rate dependence of fracture toughness than the small-grained materials do. Fig. 7(b) and (d) show that materials with blunt cracks have higher fracture toughnesses than those with sharp cracks. While this is in qualitative agreement with experimental experience, the numerical model allows the effect of the blunting radius on fracture toughness to be analyzed quantitatively. Large blunting radii must lower the stress concentration at the crack tip, which naturally leads to higher overall stresses in the material. The enhancement in fracture toughness corresponds to an increase in the number of dislocations which translates into an enlargement in the size of the plastic zone around the crack tip.

The influence of grain size on fracture toughness was of substantial interest [10]. The reader is referred to [11] for an extensive review on this topic.

Summary

The fracture toughness of rolled polycrystalline tungsten has been studied for different crack orientations over the temperature range -150 to 950°C. We found a strong anisotropy of fracture toughness and fracture behavior with respect to the rolling direction. The experimental results demonstrate the great influence of microstructure on fracture toughness and the BDT. Our first experiments at different loading rates showed that the BDTT is shifted to lower temperatures with decreasing loading rate. Furthermore, the polycrystalline material exhibits a lower loading rate dependence of fracture toughness compared to single crystals found in the literatures. This finding is also reproduced by the simulations performed by a combined approach of dislocation dynamics, cohesive zone model and a virtual dislocation based boundary element method.

References

[1] P. Gumbsch, J. Riedle, A. Hartmaier and H. F. Fischmeister: Science 282 (1998), p. 1293.

[2] J. Riedle: *Der Bruchwiderstand in Wolfram-Einkristallen: Einfluss der kristallographischen Orientierung, der Temperatur und der Lastrate* (VDI Verlag, Germany 1995).

[3] A. Giannattasio and S. G. Roberts: Phil. Mag. A 87 (2007), p. 2589.

[4] M. Faleschini, H. Kreuzer, D. Kiener and R. Pippan: J. Nucl. Mater. 367-370 (2007), p. 800.

[5] N. C. Broedling, A. Hartmaier, and H. J. Gao: Int. J of Fract., 140:169–181,

[6] X.H. Zeng and A. Hartmaier, Modeling size effects on fracture toughness in semi-brittle crystals by dislocation dynamics, *to be published*

[7] P. Norajitra, A. Gervash, R. Giniyatulin, T. Ihli, W. Krauss, R. Krussmann, V. Kuznetsv, A. Makhankov, I. Mazul, and I. Ovchinnikov: Fusion Eng. Des. 81(2006), p. 341.

[8] T. Nishida, G. Pezzotti, T. Mangialardi, and A. E. Paolini, Fract. Mech. Ceram. 11 (1996), p. 107.

[9] A. Hartmaier and P. Gumbsch: Phys. Rev. B, 71:024108–1 to 024108–11, 2005.

[10] E.Werner: Z. Metallkd., 79:585–590, 1988.

[11] Z. Fan: Mater. Sci. and Eng. A, 191:73–83(11), 1995.